Schizophrenia Research 214 (2019) 24–33

Contents lists available at ScienceDirect

Schizophrenia Research

journal homepage: www.elsevier.com/locate/schres

Effective connectivity within a triple network brain system discriminates schizophrenia spectrum disorders from psychotic bipolar disorder at the single-subject level

Lena Palaniyappan [a,b,c,*,1], Gopikrishna Deshpande [d,e,f,*,1], Pradyumna Lanka [d], D. Rangaprakash [d,g], Sarina Iwabuchi [h], Susan Francis [i], Peter F. Liddle [h]

[a] Department of Psychiatry, University of Western Ontario, London, ON, Canada
[b] Robarts Research Institute, University of Western Ontario, London, ON, Canada
[c] Lawson Health Research Institute, London, ON, Canada
[d] AU MRI Research Center, Department of Electrical and Computer Engineering, Auburn University, Auburn, AL, USA
[e] Department of Psychology, Auburn University, Auburn, AL, USA
[f] Alabama Advanced Imaging Consortium, Auburn University and University of Alabama Birmingham, AL, USA
[g] Department of Psychiatry and Biobehavioral Sciences, University of California Los Angeles, Los Angeles, CA, USA
[h] Centre for Translational Neuroimaging, Division of Psychiatry & Applied Psychology, Institute of Mental Health, University of Nottingham, UK
[i] Sir Peter Mansfield MR Centre, University of Nottingham, UK

ARTICLE INFO

Article history:
Received 27 September 2017
Received in revised form 8 January 2018
Accepted 11 January 2018
Available online 3 February 2018

Keywords:
Effective connectivity
Granger causality
Support vector machine
Pattern classification
Psychosis

ABSTRACT

Objective: Schizophrenia spectrum disorders (SSD) and psychotic bipolar disorder share a number of genetic and neurobiological features, despite a divergence in clinical course and outcome trajectories. We studied the diagnostic classification potential that can be achieved on the basis of the structure and connectivity within a triple network system (the default mode, salience and central executive network) in patients with SSD and psychotic bipolar disorder.

Methods: Directed static connectivity and its dynamic variance was estimated among 8 nodes of the three large-scale networks. Multivariate autoregressive models of deconvolved resting state functional magnetic resonance imaging time series were obtained from 57 patients (38 with SSD and 19 with bipolar disorder and psychosis). We used 2/3 of the patients for training and validation of the classifier and the remaining 1/3 as an independent hold-out test data for performance estimation.

Results: A high level of discrimination between bipolar disorder with psychosis and SSD (combined balanced accuracy = 96.2%; class accuracies 100% for bipolar and 92.3% for SSD) was achieved when effective connectivity and morphometry of the triple network nodes was combined with symptom scores. Patients with SSD were discriminated from patients with bipolar disorder and psychosis as showing higher clinical severity of disorganization and higher variability in the effective connectivity between salience and executive networks.

Conclusions: Our results support the view that the study of network-level connectivity patterns can not only clarify the pathophysiology of SSD but also provide a measure of excellent clinical utility to identify discrete diagnostic/prognostic groups among individuals with psychosis.

1. Introduction

The two major psychotic disorders, schizophrenia and bipolar disorder with psychosis, display more shared than unique abnormalities in brain structure (Ellison-Wright and Bullmore, 2010; Maggioni et al., 2017; Nenadic et al., 2015b, 2015a; Nenadić et al., 2017b), function (Sui et al., 2011; Baker, 2014) and candidate genetic loci (Craddock and Owen, 2010; Lichtenstein et al., 2009). Despite this similarity, the clinical course and functional outcome of these disorders are notably divergent (Demjaha et al., 2011; Murray et al., 2004). The early conceptualization of schizophrenia placed emphasis on certain features (the predominance of poor functional outcome, the absence of clearly defined periods of complete remission, and the presence of thought disorder (disorganization)) as cardinal to define its distinctive phenotype (Ketter et al., 2004), though in clinical practice these are insufficient to

* Corresponding authors.
E-mail addresses: lpalaniy@uwo.ca (L. Palaniyappan), gopi@auburn.edu (G. Deshpande).
[1] Equal contribution.

https://doi.org/10.1016/j.schres.2018.01.006
0920-9964/

confidently separate the two major psychotic disorders. Clarifying the neuroanatomical basis of the distinction between these two disorders can greatly enhance our understanding of the pathophysiological core of schizophrenia.

In recent times, the concept of dysconnectivity based on functional imaging (fMRI) has provided a robust framework to study the dysfunctional interaction among anatomically distinct brain regions (Friston, 1994). A large body of literature supports the notion of widespread functional dysconnectivity in psychosis (Pettersson-Yeo et al., 2011). An elegant model of dysconnectivity involving large-scale brain networks – Triple Network Model – was recently proposed by Menon (2011). This model places emphasis on the default mode network (comprising of the ventral medial prefrontal cortex [vMPFC] and posterior cingulate cortex [PCC]), central executive network (dorsolateral prefrontal cortex [DLPFC] and posterior parietal cortex [PPC]) and the salience network (right frontoinsular cortex [rFIC] and dorsal anterior cingulate cortex [dACC]) (Seeley et al., 2007). The development of the triple-network model was based on a Granger-causal fMRI connectivity study that reported the primacy of the salience network in influencing the other two networks during task processing (Sridharan et al., 2008). Subsequently, several Granger-causal fMRI studies have provided empirical support for aberrant effective connectivity (i.e. connectivity with causal directionality information included, as opposed to functional connectivity where no directional information can be inferred) among these three networks in schizophrenia when compared to healthy controls (Manoliu et al., 2013a, 2013b; Moran et al., 2013; Palaniyappan et al., 2013). We reported that in patients with schizophrenia and schizoaffective disorder (schizophrenia spectrum disorders (SSD)), right anterior insula fails to influence DLPFC and this pattern was related to the overall burden of psychotic symptoms and the functional outcome in clinically stable, medicated subjects with SSD (Palaniyappan et al., 2013). To date, only a few studies have examined the differential patterns of connectivity in bipolar disorder and SSD with some (Calhoun et al., 2012; Chai et al., 2011; Mamah et al., 2013) but not all (Argyelan et al., 2013; Baker, 2014) reporting specific spatial patterns of dysconnectivity. Despite methodological differences, there is some agreement on the presence of connectivity differences separating the two psychotic disorders that involve the medial prefrontal cortex (Calhoun et al., 2012; Chai et al., 2011) and the insula (Calhoun et al., 2012; Mamah et al., 2013). Interestingly, these brain regions also show a substantial reduction in grey matter volume in psychosis (Glahn et al., 2008). To date, no study has investigated the differences in effective ('causal') connectivity strength or their dynamic (temporal) variability within the triple network framework in the two diagnostic groups.

Multivariate pattern classification approaches provide the diagnostic test accuracy measures using information derived from a large number of clinical and imaging variables (Deshpande et al., 2013; Libero et al., 2015). Our clinical diagnostic ability can be significantly improved using this approach (Iwabuchi et al., 2013). The use of pattern classification approaches on structural neuroimaging measures has successfully discriminated bipolar disorder from SSD (Nenadić et al., 2017a; Salvador et al., 2017; Schnack et al., 2014). In the present study, within the triple network framework, we use connectivity-based information from Granger-causal analysis of resting-state fMRI, grey matter volume of the relevant brain regions from structural imaging, and the readily available clinical information from symptom clusters (reality distortion, psychomotor poverty, disorganization) in 38 patients with SSD (reported previously (Palaniyappan et al., 2013)) and 19 patients with bipolar disorder and psychosis. Using 5 different classification algorithms based on diverse principles and a consensus classifier which combines the predictive abilities of the individual classifiers, we investigated whether these approaches could provide sufficient accuracy either independently or in combination to discriminate an individual with SSD from another with psychotic bipolar disorder.

2. Methods

2.1. Participants

The sample consisted of 38 patients satisfying DSM-IV criteria for SSD and 19 subjects with psychotic bipolar disorder. Patients were recruited from the community-based mental health teams (including Early Intervention in Psychosis teams) in Nottinghamshire and Leicestershire, UK. The diagnosis was made in a clinical consensus meeting in accordance with the procedure of Leckman et al. (1982), using all available information including a review of case files and a standardized clinical interview (SSPI) (Liddle et al., 2002). All patients were in a stable phase of illness (defined as a change of no more than ten points in their Global Assessment of Function [GAF] score, assessed 6 weeks prior and immediately prior to study participation). The patient group with SSD has been previously reported in our earlier study (Palaniyappan et al., 2013). While schizoaffective illness is often considered an indeterminate diagnostic category, most neurocognitive and neuroimaging observations (Amann et al., 2016; Madre et al., 2016; Ramón Landin-Romero et al., 2017) call for schizoaffective illness to be considered as a subtype of schizophrenia, though notable exceptions are reported (Nanda et al., 2014). Consequently, we followed the continuum model of bipolar disorder and schizophrenia used by most neuroimaging studies to date (Birur et al., 2017) and included subjects with schizoaffective disorder in the same category as schizophrenia (SSD). The study was given ethical approval by the National Research Ethics Committee, Derbyshire, UK. All volunteers gave written informed consent. Clinical and demographic characteristics of this sample are presented in Table 1.

2.2. Clinical assessment

Patients were interviewed on the same day as the scan by a research psychiatrist (LP and VB) to assess the clinical severity of Reality Distortion, Psychomotor Poverty and Disorganisation over the previous week

Table 1
Demographic and clinical features.

	Patients with bipolar disorder (n = 19)	Patients with schizophrenia (n = 38)	t or chi-square value/p
Gender (male/female)	13/6	29/9	x2 = 0.41, p = .52
Handedness (right/left)	17/2	33/5	x2 = 0.08, p = .78
Age in years (SD)	34.53(10.5)	34.53(9.1)	t = 0, p = 1
Mean duration of illness in years (SD)	10.5(8.2)	9.8(7.7)	t = 0.33, p = .74
SOFAS score	62.4(15.2)	53.9(12.8)	t = 2.2, p = .03
Mean parental NS-SEC (SD)	1.8(1.2)	2.4(1.5)	t = 1.33, p = .27
Mean total SSPI score	7.4(8.2)	11.9(7.4)	t = 2.1, p = .04
Reality distortion	0.58(1.4)	2.26(2.6)	t = 2.6, p = .01
Disorganization	0.32(1.0)	1.39(1.3)	t = 3.2, p = .003
Psychomotor poverty	1.26(2.1)	2.84(3.6)	t = 1.8, p = .08

NS-SEC: National Statistics – Socio Economic Status; SD: standard deviation; SSPI – Symptoms and Signs of Psychotic Illness. The total SSPI score can vary between 0 and 80. Reality distortion (delusions and hallucinations) can vary between 0 and 8. Psychomotor poverty (anhedonia, underactivity, poverty of speech and flat affect) can vary between 0 and 16. Disorganization (inappropriate affect, disordered thought form and poor attention) can vary between 0 and 12.

using the SSPI. Duration of illness was calculated from the retrospective assessment of the time of onset of the index episode of the illness (mean (SD) bipolar group = 10.5(8.3) years; SSD = 9.8(7.73) years). Social and occupational dysfunction was quantified using the SOFAS scale ((American Psychiatric Association, 1994)). 54 out of 57 patients were receiving psychotropic medications at the time of scan. We calculated the median Defined Daily Dose (DDD) separately for antipsychotics, mood stabilizers (including lithium), and antidepressants (WHO Collaborating Centre for Drug Statistics and Methodology, 2003). A detailed breakdown of the prescribed medications is presented in the Supplement.

2.3. MRI data acquisition

Functional MRI images were acquired on a 3 Tesla Philips Achieva MRI scanner (Philips, Netherlands) during 10 min of rest, with eyes open. We acquired dual-echo gradient-echo echo-planar images (GE-EPI) to enhance sensitivity and reduce susceptibility effects (2), using an eight-channel SENSE head coil with SENSE factor 2 in anterior–posterior direction, TE1/TE2 25/53 ms, flip angle 85°, 255 × 255 mm field of view, with an in-plane resolution of 3 mm × 3 mm and a slice thickness of 4 mm, and TR of 2500 ms. At each dynamic time point a volume dataset was acquired consisting of 40 contiguous axial slices acquired in descending order. 240 time points were acquired during the resting fMRI paradigm. A magnetization prepared rapid acquisition gradient echo image with 1 mm isotropic resolution, 256 × 256 × 160 matrix, TR/TE 8.1/3.7 ms, shot interval 3 s, flip angle 8°, SENSE factor 2 was also acquired. The sequences were inspected upon acquisition, and repeated if obvious movement effects were noted.

2.4. Data analysis

SPM8 (http://www.fil.ion.ucl.ac.uk/spm) and Data Processing Assistant for resting-state fMRI (Chao-Gan and Yu-Feng, 2010) softwares were used for fMRI preprocessing. After slice-timing correction, images were spatially realigned to the first image of the data set. Movement parameters were assessed for each participant, and participants were excluded if movement exceeded 3 mm. In addition, ArtRepair, a scrubbing procedure, was employed to correct framewise displacement motion artifacts using an interpolation method (http://cibsr.stanford.edu/tools/human-brain-project/artrepair-software.html). The first five volumes of functional images were discarded to allow stability of the longitudinal magnetization. Weighted summation of the dual-echo images produced a single set of low-artifact functional images (Posse et al., 1999). Retrospective physiological correction was then performed (Glover et al., 2000), followed by spatial normalization using the unified segmentation approach and smoothed using a Gaussian kernel of 8 mm full-width at half- maximum. Linear detrending was done followed by filtering using a band-pass filter (0.01–0.08 Hz). Variance accounted for by nuisance covariates including six head motion parameters, global mean signal, white-matter signal, and CSF signal was removed. Removal of global signal has been shown to reduce physiological noise from resting fMRI (Fox et al., 2009; Hayasaka, 2013; Yan et al., 2013), though negative values of connectivity must be cautiously interpreted (Chang and Glover, 2009).

2.5. Seed regions

The seed regions representing the three networks (SN, DMN and CEN) were selected in line with Shridharan et al. (Sridharan et al., 2008), who identified maximal peak activation and deactivation loci from task fMRI data on subjects who also underwent resting state fMRI. Using functional activation data during a two-back task performed by all subjects included in the study (one-sample *t*-test, familywise error [FWE] corrected $p < .05$), seed regions corresponding to bilateral insula and ACC (3 regions for the SN), right DLPFC and bilateral PPC (3 regions for CEN), VMPFC and PCC (2 regions for DMN) were identified (Table 2). A 6 mm radius sphere centered on each of the local maxima was used to extract time series of BOLD signals.

2.6. Connectivity analysis

The mean time series from 8 ROIs were obtained for each of the 57 participants (19 Bipolar and 38 SSD participants). These time series were normalized and deconvolved using the blind deconvolution technique proposed by Wu et al. (2013) to obtain the underlying latent neuronal variables, which were then input into the MVAR model to obtain two types of Granger causal metrics between the 8 ROIs for all the participants. First, we estimated static effective connectivity (SEC), which is the conventional Granger causality measure obtained in terms of a single Multivariate autoregressive (MVAR) model coefficient per run/subject (Liang et al., 2014). MVAR models have been used in numerous earlier studies (Abler et al., 2006; Deshpande et al., 2008, 2009, 2010, 2011, 2012; Deshpande and Hu, 2012; Hampstead et al., 2011; Krueger et al., 2011; Lacey et al., 2011; Preusse et al., 2011; Roebroeck et al., 2005; Sathian et al., 2011; Strenziok et al., 2011) to characterize the predictive relationship between the time series from different regions of the brain. We also used a second type of Granger causal metric - the variance of the dynamic effective connectivity (Hutcheson et al., 2015; Wang et al., 2017; Wheelock et al., 2014) (vDEC). The coefficients of the MVAR model were allowed to vary as a function of time to obtain an effective connectivity value for each time point for every run/subject (Feng et al., 2016; Goodyear et al., 2017; Grant et al., 2014). The variance of the DEC time series (vDEC) was then obtained to charactize the temporal variability of effective connectivity over the duration of the experiment (Rangaprakash et al., 2017). For each possible path between the 8 ROIs, *t*-tests were performed between SSD and the bipolar groups and those paths which had significantly different SEC and vDEC ($p < .05$) between the groups were obtained. More details of the Effective Connectivity Model is provided in the Supplementary material.

2.7. Morphometry analysis

One patient with SSD and one patient with bipolar disorder were excluded from the morphometry analysis due to poor image quality, resulting in a total of 37 patients with SSD and 18 patients with psychotic bipolar disorder. The T1 MPRAGE images were resliced and segmented into grey, white and CSF tissue using the SPM8 Diffeomorphic Anatomical Registration Through Exponentiated Lie algebra (DARTEL) algorithm (Ashburner, 2007). The grey matter images were bias field

Table 2
Regions of interest representing the nodes of three large-scale networks.

Network	Region	Coordinates used by Sridharan et al. (2008) (in mm)	Coordinates used in this study (in mm)
Salience network	Right fronto-insular cortex (RFIC)	37, 25, −4	33, 21, −3
	Left Fronto-Insular Cortex (LFIC)	−32, 24, −6	−33, 21, −3
	Anterior cingulate cortex (ACC)	4, 30, 30	6, 15, 42
Central executive network	Dorsolateral prefrontal cortex (DLPFC)	45, 16, 45	45, 3, 42
	Right Posterior Parietal Cortex (RPPC)	54, −50, 50	42, −45, 39
	Left Posterior Parietal Cortex (LPPC)	−38, −53, 45	−30, −54, 42
Default mode network	Ventromedial Prefrontal Cortex (vMPFC)	−2, 36, −10	0, 60, 3
	Posterior cingulate cortex (PCC)	−7, −43, 33	3, −48, 24

corrected to reduce field inhomogeneity, warped onto a group average template and normalized to MNI space. Images were smoothed using an 8 mm FWHM isotropic Gaussian kernel. For each subject, we extracted the mean volumes for each of the 8 seed regions from all voxels that were included in the spherical ROI masks described above.

2.8. Classification analysis

We divided the total data into two homogenous samples, matched for age and gender. The first data sample consisting of data from 38 subjects (67% of the total data) was used for training/validation. It should be noted that even though we calculated connectivity measures from all the subjects, we used just the training/validation data for feature selection and reporting the unbiased cross-validation accuracy. Within the training/validation data, we performed a nested cross-validation procedure, with the inner cross-validation loop for feature selection and an outer cross-validation loop for performance estimation. In order to validate our classification performance, we used the remaining 19 subjects (33% of the total data) as an independent hold-out test dataset. The hold-out test data was untouched for feature selection and elimination. The features removed from the training/validation dataset were also removed from the hold-out test dataset for prediction, though we used just the training/validation dataset for feature selection and elimination. Using the classifier models obtained from the training/validation data, we predicted the class labels on the hold-out test data by a majority voting procedure as described later. By separating the training/validation and the hold-out test-data at every level of analysis, we ensured that double dipping was prevented in our analyses. Three sets of features: (1) The static effective connectivity (SEC) and the variance of dynamic effective connectivity (vDEC) from all 56 paths involving the 8 nodes in each subject of both groups leading to a total of 112 effective connectivity metrics, (2) SSPI scores on reality distortion, disorganization and psychomotor poverty, (3) Grey matter volume estimates of the 8 seed regions based on VBM analysis, were used to train and validate the classifiers.

Earlier studies have shown that classification can be enhanced by iteratively removing non-discriminatory features (Craddock et al., 2009). In this regard, filtering and wrapper methods have been used to improve the performance of the classifier. Filtering methods select the features that are statistically different between the classes based on statistical tests such as a *t*-test. The wrapper methods such as recursive feature elimination (RFE) and recursive cluster elimination (RCE) minimize prediction error by the iterative elimination of unwanted features. RCE is one such wrapper method in which feature elimination and classification steps are embedded with each other in an iterative fashion. We used 5 different classifiers implemented within a recursive cluster elimination (RCE) framework (Yousef et al., 2007) to classify the subject categories. The classifiers we used were (1) Extreme Learning Machines (ELM) (Huang et al., 2011), (2) K-Nearest Neighbors (KNN), (3) Linear Discriminant Analysis (LDA), (4) Linear Support Vector Machine (L-SVM), and (5) RBF-kernel Support Vector Machine (RBF-SVM). A description of the methods can be found in James et al. (2013). These classifiers were specifically chosen given their popularity, computational speed, relative lack of sensitivity to smaller sample size and their ability to being embedded within an RCE framework which allows for discriminative features to be inferred.

We obtained the cross-validation accuracy by training and validating our classifier models on the training/validation data consisting of 38 subjects. The classifier models which were obtained from the training/validation data were saved and used to vote on the hold-out test data containing 19 subjects to give us the hold-out test accuracy on an independent dataset to validate our classification performance as mentioned earlier. The flow chart in Fig. 1 illustrates the main steps of the classification framework. More information about the classification procedure can be found in the supplementary material. For all the classifiers, we report both the balanced and unbalanced accuracies due to class imbalances in the number subjects with Bipolar disorder with Psychosis and SSD in our dataset. The balanced accuracy is the mean of individual class accuracies. Using the saved decision boundaries of the 5 classifiers, we combined the predictions of the each of the classifier weighted by their cross-validation classification accuracy, to predict the class labels on the hold-out test data. This consensus classifier approach avoids the limitations of any individual classifier as different classifiers follow different underlying principles for classification All machine learning classifiers have an inductive bias which indicate the set of assumptions the classifier makes about the relationship between inputs and output. Since, we do not know the underlying relationship between the inputs and the output, combining the predictions of multiple classifiers by weighing them by their balanced CV accuracy obtained from the training/validation data could give us a better performance than any individual classifier. It also ensures complete separation between the training/validation data and test-data, thus preventing double dipping.

2.9. Follow-up tests and correlation analyses

All classifiers implemented within the RCE framework provided us with scores for features which indicate their ability to discriminate between the two disorders. Therefore, we calculated the weighted accuracy of the feature discriminability scores for all the 5 classifiers and calculated a final consensus score to identify important predictors. Since the RCE-framework also included an inbuilt *t*-test (uncorrected $p < .1$) on the predictors in training/validation data, the predictors we identified based on the consensus scores not only had predictive value at the single subject level, but were also statistically separated between the two groups, at the group-level to some extent. The reason for not using a stricter threshold was that it could lead to removal of a lot of features in the smaller dataset, which might otherwise have predictive ability as statistical significance is not a good indicator of the predictive ability of a feature. Secondly, we studied the relationship between the symptom scores and the predictors identified above (SEC, vDEC or grey matter values) that separated the two disorders using Spearman's correlation (uncorrected $p < .05$). Correlation analysis was performed separately for each diagnostic group. In addition, we also studied the influence of prescribed dose of antipsychotics in both groups, and of antidepressants and mood stabilizers in bipolar disorder on the effective connectivity coefficients. A wider exploratory correlational analysis testing the symptom relationship for all 56 paths is reported in the Supplement.

3. Results

3.1. Group differences

The paths within the triple network system showing significant group differences for SEC and vDEC are listed in Table 3 and shown in Fig. 2. This demonstrates reduced (and predominantly negative) cross network connectivity strength in SSD subjects compared to the bipolar subjects, primarily from salience to default mode network, executive control to default mode network, as well as within the salience network. On the other hand, the output from the default mode network into salience and executive networks were positive and stronger in the SSD group. However, the connectivity was significantly more variable over time in SSD as compared to bipolar in bidirectional interactions between the salience and executive control networks.

3.2. Classification results

A cross-validation accuracy of 61.8% −76.3% was noted for the individual classifiers, with the highest accuracy obtained using the methods ELM, L-SVM and RBF-SVM. The classification results are shown in Table 4. Since the number of patients with SSD and Bipolar disorder was not equal in the dataset, we also report the balanced accuracy (mean of individual class accuracies) for all the classifiers. We got

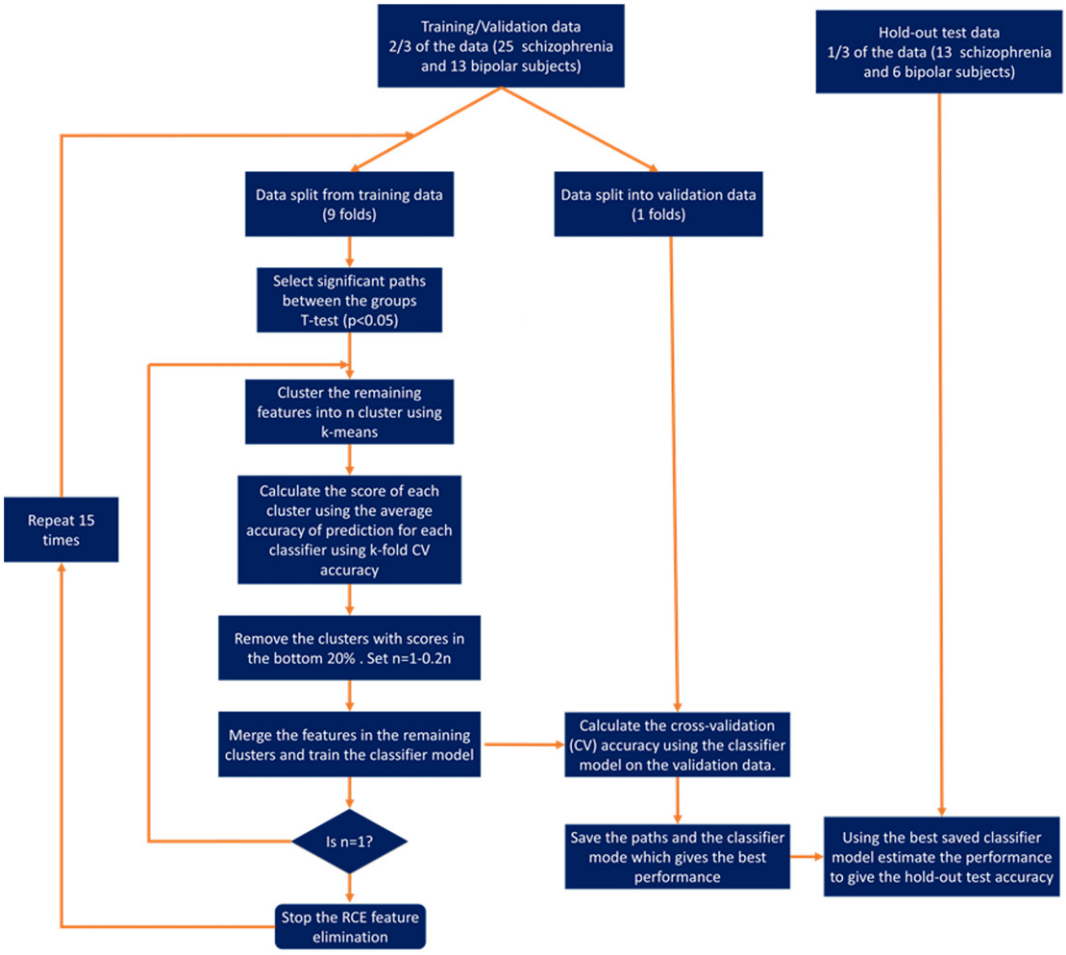

Fig. 1. A schematic illustrating the RCE algorithm for classification of SSD and bipolar disorder subjects.

excellent performance with the consensus classifier with an overall accuracy of 94.7% (unbalanced) and 96.2% (balanced) on the independent hold-out test data. We obtained individual class accuracies of 100% and 92.3% for Bipolar disorder and SSD, respectively. The confusion matrices associated with the performance of the classifiers on the hold-out test dataset is shown in Table S5. The top 10 features as identified by the RCE framework are displayed in Table 5 along with their rank (which indicates their discriminative ability). Results of the follow-up *t*-tests and symptom correlations are also shown in Table 5.

3.3. Euclidean distance

It is noteworthy that certain features, such as vDEC of the path LPPC → LFIC, correlated with reality distortion in both groups while not being

Table 3
Mean value and standard deviation of the effective connectivity metrics for the paths that are significantly different ($p < .05$) between the bipolar and schizophrenia groups.

Static effective connectivity					
Paths significantly greater in bipolar group compared to Schizophrenia spectrum disorder group					
Source region	→	Sink region	SEC values: bipolar (mean ± std)	SEC values: Schizophrenia (mean ± std)	*t*-Test p-value
LFIC	→	vMPFC	0.03 ± 0.065	−0.11 ± 0.085	0.0015
LFIC	→	PCC	−0.03 ± 0.055	−0.11 ± 0.075	0.0352
LPPC	→	PCC	0.1 ± 0.1	−0.02 ± 0.115	0.0449
RFIC	→	ACC	0.16 ± 0.165	−0.02 ± 0.14	0.0455
Paths significantly greater in Schizophrenia group compared to bipolar group					
Source region	→	Sink region	SEC values: bipolar (mean ± std)	SEC values: Schizophrenia (mean ± std)	*t*-Test p-value
PCC	→	LPPC	−0.13 ± 0.095	0.02 ± 0.115	0.0112
vMPFC	→	LFIC	0.00 ± 0.055	0.09 ± 0.09	0.0121
Variance of dynamic effective connectivity					
Paths significantly greater in Schizophrenia spectrum disorder group compared to bipolar group					
Source region	→	Sink region	vDEC values: bipolar (mean ± std)	vDEC values: Schizophrenia (mean ± std)	*t*-Test p-value
LFIC	→	RPPC	0.11 ± 0.02	0.15 ± 0.03	0.0074
DLPFC	→	RFIC	0.12 ± 0.02	0.17 ± 0.04	0.0084

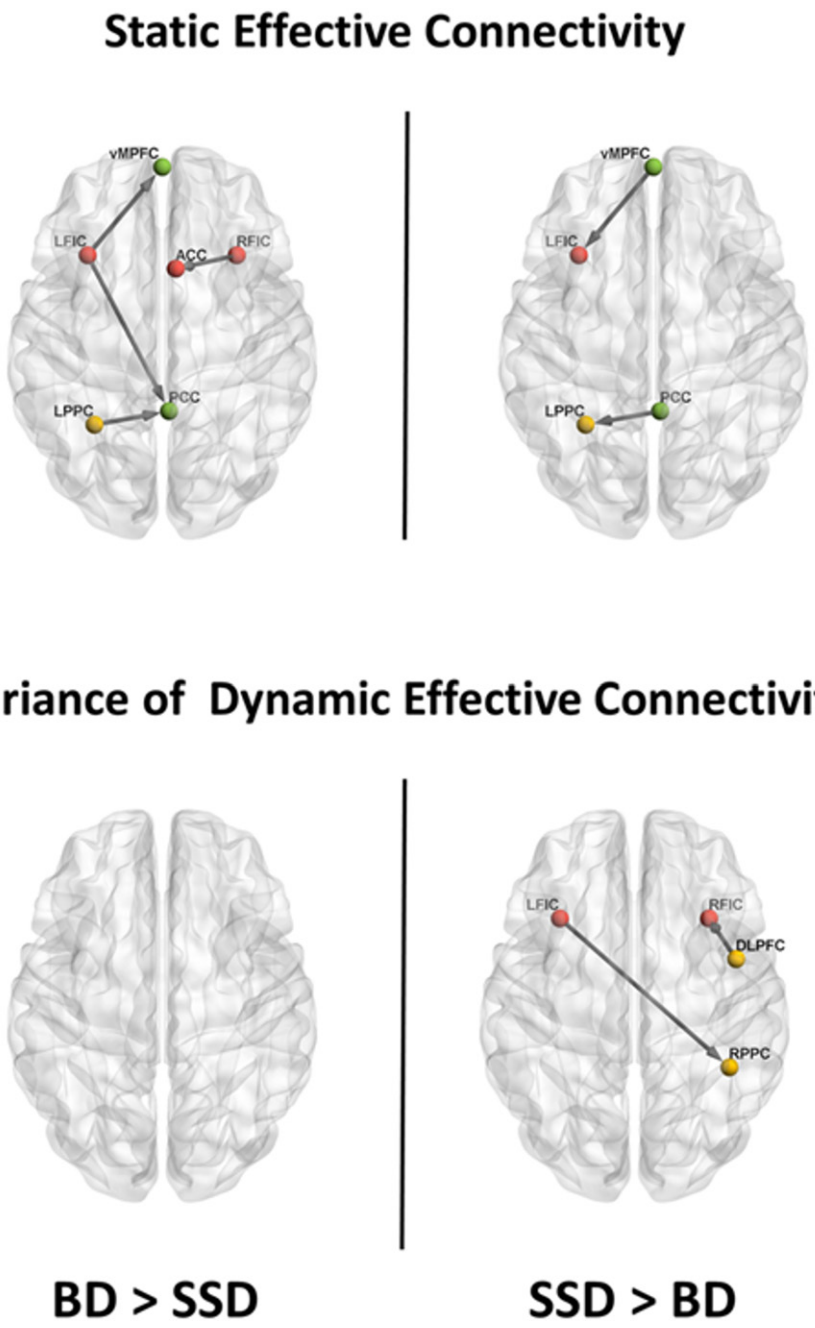

Fig. 2. (left) Paths significantly stronger in bipolar participants compared to SSD participants. (right) Paths significantly stronger in SSD participants compared to bipolar participants. The color of the node indicates the network the ROI belongs to: Green – Default mode network; Red – Salience network; Yellow – Central executive network. The color and width of the paths indicate the p-value of the between group comparison BD – Bipolar disorder group; SSD- Schizophrenia spectrum disorder group.

Table 4
Classification performance of the classifiers we used, along with the performance of the consensus classifier on the hold-out test data. We used grey matter volume, SEC and vDEC within the triple network, and symptom scores as features.

Classifiers	Cross-validation accuracy				Hold-out test accuracy			
	Unbalanced	Balanced	Bip	SSD	Unbalanced	Balanced	Bip	SSD
ELM	66.7%	62.7%	50.3%	75.2%	73.7%	67.3%	50%	84.6%
KNN	76.3%	82%	100%	64%	63.2%	64.1%	66.7%	61.5%
LDA	61.8%	54.8%	32.8%	76.8%	73.7%	67.3%	50%	84.6%
L-SVM	76.3%	82%	100%	64%	63.2%	64.1%	66.7%	61.5%
RBF-SVM	76.3%	82%	100%	64%	63.2%	64.1%	66.7%	61.5%
Consensus	NA	NA	NA	NA	94.7%	96.2%	100%	92.3%

Bip – bipolar disorder group; SSD – Schizophrenia spectrum disorder group; NA – not applicable.

Table 5
Top features with highest discriminative power using grey matter volume, effective connectivity within the triple network, and symptom scores.

Feature	Type of effective connectivity	Classifier rank	Between group *t*-test	Symptom correlation in bipolar disorder group	Symptom correlation in SSD group	Correlation with antipsychotic dose
Disorganization	NA	1	SSD > Bip	NA	NA	NA
LPPC → LFIC	Dynamic	2	No difference	RD ($r = -0.46$, $p = .047$)	RD ($r = 0.5$, $p = .001$)	None
DLPFC → RFIC	Dynamic	3	SSD > Bip	None	None	None
ACC volume	NA	4	No difference	None	None	None
RPPC → LPPC	Dynamic	5	No difference	None	None	None
Reality distortion	NA	6	SSD > Bip	NA	NA	NA
RFIC → RPPC	Static	7	No difference	None	None	None
PCC volume	NA	8	No difference	None	None	None
LFIC → vmPFC	Static	9	Bip > SSD	None	None	None
ACC → vmPFC	Dynamic	10	No difference	None	None	None

The features are displayed in descending order of classification rank (lesser the numerical rank, more important for classification). The statistical separation of each feature between the groups as well as significant correlation of effective connectivity paths with behavioral scores in both Bipolar and Schizophrenia samples is shown. The p-values for the *t*-tests corresponding to group differences are shown in Table 3. Further information on the correlations is provided in Table 1 of the supplement. NA – not applicable; Bip – bipolar disorder group; SSD-Schizophrenia spectrum disorder group; RD – reality distortion scores.

significantly different in value between the groups. Certain features were highly ranked, but displayed no correlation with symptoms and were also not significantly different between the groups. Further, other features, predominantly the output from the salience network, were significantly different between the groups, but did not correlate with symptoms in individual groups. None of the features were correlated with the dosage of anti-psychotic medication. These observations support the notion that statistical separability of individual features at the group level is qualitatively different from the ability of features taken together for predicting the diagnostic label of individual subjects. In order to elaborate and illustrate this point, we estimated the Euclidean distance between the feature values obtained from both the groups. We started from the top-ranked feature and identified the Euclidean distance between feature clusters (corresponding to the two groups) by successively adding lower ranked features into the clusters. The change in Euclidean distance with additional features informs us about the discriminative ability contributed by the addition of the new feature, in combination with the features that already exist within the cluster. Fig. 3 shows the Euclidean distance between the cluster means of the normalized features for Bipolar disorder and SSD as a function of the features. As the figure illustrates, the Euclidean distance increases as more and more informative features are added (note that the uninformative features have already been eliminated using the RCE algorithm), thus increasing the seperability between the classes.

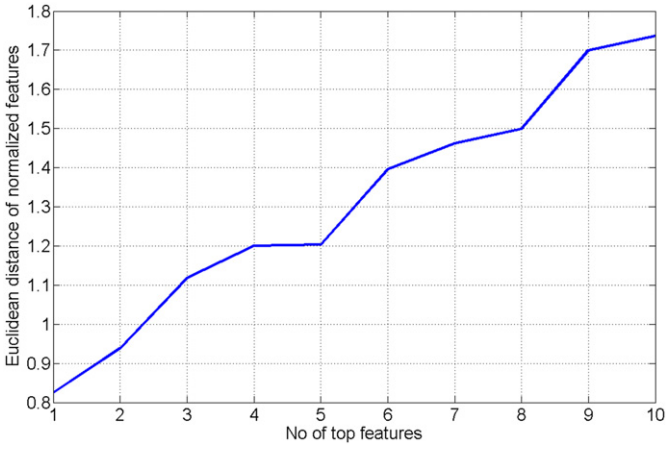

Fig. 3. Plot showing the change in the Euclidean distance between cluster centers of the normalized values of the features for Bipolar disorder and SSD as the features are added. The increase in the Euclidean distance is shown for the top 10 features. Note that each point on the x-axis indicates the rank of the feature being added to the pre-existing cluster. The features corresponding to the rank values are shown in Table.5. For example, #4 on the x-axis indicates that the SSD and Bipolar clusters contained values from feature # 1,2,3 and 4. The increase in Euclidean distance from # 3 to # 4 demontrates that addition of feature #4 to the pre-existing cluster (containing features 1,2 and 3) increased the separability between the groups.

4. Discussion

Using Granger-causal fMRI analysis for the first time to study the differences in brain connectivity between SSD and psychotic bipolar disorder, we report 3 major observations: (1) Very high (96.2%) cross-validation accuracy separating the two illnesses was achieved using a combination approach, while the individual classifiers provided only 61.8% −76.3% accuracy. (2) Significant differences between the 2 diagnostic groups in the effective connectivity within the triple network system (3) Clinical symptoms that persisted despite treatment make an important contribution to the accuracy of discriminating the 2 major psychotic disorders - bipolar disorder and SSD. While previous studies (Arribas et al., 2010; Koutsouleris et al., 2015; Salvador et al., 2017; Schnack et al., 2014) employed a whole brain approach without selecting brain regions a priori when seeking diagnostic separation of SSD and bipolar disorder, we utilized a biomodel (triple network abnormalities) to inform the classification process, resulting in a notable gain in test performance measures. Such model-based approach also allowed us to utilize effective connectivity (static or dynamic) in a pattern classification framework for the first time to separate patients with SSD from those with bipolar disorder.

It is important to note that even though certain features were themselves not significantly different between the groups in their own right, they increased separability between the groups when used in combination with other features. This emphasizes the strength of the multivariate nature of classifier models in discriminating bipolar disorder and SSD, consistent with several previous studies (Arribas et al., 2010; Calhoun et al., 2008; Costafreda et al., 2011; Koutsouleris et al., 2015; Salvador et al., 2017; Schnack et al., 2014). Using the consensus approach for classifiers, we correctly identified all of the patients with bipolar disorder (100% class accuracy) and 92.3% of those with SSD. This accuracy is greater than the discriminability noted by other groups, though the samples studied by others included both type 1 and 2 bipolar disorder (Schnack et al., 2014) and a number of subjects with bipolar disorder but no psychotic symptoms (Arribas et al., 2010; Costafreda et al., 2011; Koutsouleris et al., 2015; Schnack et al., 2014).

To our knowledge, for the first time, we have demonstrated the utility of combining clinical ratings with neuroimaging measures to separate SSD from psychotic bipolar disorder. Most prior studies employing multivariate machine learning approaches have either utilized clinical measures or imaging measures alone, without testing the value of combining them. Given that the correlation reported between symptoms and imaging meaures in general are only modest in psychiatric illnesses

(Mathalon and Ford, 2012), the higher accuracy achieved using a combination approach is not surprising. We note that the severity of disorganization (Table 5), considered by some as the central aspect of SSD (Taylor et al., 2010), was the top contributor to the discrimination accuracy. Interestingly, the earliest notions of SSD proposed by Bleuler (1950) focused on disorganization (loosening of association) as a primary feature of this illness. It is important to note that the patients in this sample were medicated and were clinically and functionally stable i.e. not acutely psychotic. In this context, the symptom scores indicate the non-responsive aspect of the illness.

Patients with SSD display a pattern of connectivity that indicates a significant reduction in the interaction among the triple networks (Table 3). These results are consistent with a large body of literature, including our own work, highlighting the triple network dysfunction in SSD, with a central role for the salience network. Transdiagnostic aberrations in the triple network system, as demonstrated recently (Sheffield et al., 2017), is consistent with the physiological role of the triple network system in healthy cognitive performance. Nevertheless, our observations point to certain diagnostic specificity in the pathways that fail within this sytem The most significant differences in patients with SSD when compared to patients with bipolar disorder involved (1) the significant instability (i.e. higher variability in DEC) of the influence between the salience and the executive network and (2) the reduced influence from the salience to default mode network (LFIC to vMPFC and LFIC to PCC). Thus, fractionation of directional influences within the triple network system yields diagnostic information in psychosis that holds important translational value (Palaniyappan et al., 2017).

Several limitations must be borne in mind when interpreting these results. A classification accuracy of 94.7% has been achieved in a sample of clinically stable, medicated patients with psychosis, with a mean duration of illness > 10 years. The real-world utility of this approach needs to be tested in a first episode sample where exposure to medication is minimal and the discriminatory ability based solely on clinical symptoms is poor. Nevertheless, as symptom scores synergise with the triple network connectivity metrics to improve the accuracy, we could expect a better if not the same classifying ability in a highly symptomatic, unmedicated first episode sample. There are various means of quantifying effective connectivity using fMRI, though all of these suffer from certain methodological limitations. Interpreting neural connectivity from fMRI has certain limitations, discussed at length in our previous work. By employing deconvolved fMRI data, we have addressed some of those limitations. In brief, when two groups are compared, differences in Granger causal coefficients provide a meaningful measure of pathophysiology, even if the source of such differences is not fully known. Further, we used a correlation-purged Granger causal model on deconvolved fMRI data, which has the advantage of being more readily interpretable at a neuronal level (Deshpande et al., 2011).

A significant limitation of our study as well as many other studies using clinical datasets is the small sample size. Overfitting can be a huge problem in small datasets. So we used a hypothesis driven study, where we restricted our focus to MRI measures of 8 ROIs (their pairwise dynamic connectivity measures and grey matter volumes), as well as the symptom scores. This adds up to a total of 123 features which is still large compared to the number of subjects with Bipolar and SSD. Therefore, we further performed a feature selection to reduce any overfitting and work in lower-dimensional space. Also, small samples limits our ability to capture the heterogeneity of the disease populations. It is exactly for this reason that we have used an independent test data. Accuracies associated with this provide a conservative lower bound which could be substantially improved using a larger and heterogeneous data sets. Our results must be further replicated with a larger samples.

Effective connectivity within the triple network system, when used in conjunction with clinical assessment, accurately classified patients with SSD from those with psychotic bipolar disorder, and correlated with reality distortion. This not only underscores the importance of the dynamic imbalance within the triple network system in explaining the phenomenological core of SSD but also raises the question of utilizing this framework for diagnostic/prognostic purposes when an individual presents with psychotic symptoms. Neuroimaging, when used alongside clinical assessment, can provide an objective means to aid differential diagnosis and clinical decision making.

Acknowledgment

Funding: This work was funded by the Medical Research Council (UK) Grant Number: G0601442. L Palaniyappan is supported by the Canadian Institute of Health Research (Foundation Grant 375104), Bucke Family Fund and the Academic Medical Organization of South Western Ontario.

Role of funding sources

The funders had no role in the design of experiments, analysis of data, interpretation of the results or the decision to publish the findings.

Contributors

LP and PFL designed the study; LP, SF & PFL collected the data from University of Nottingham. GD planned the analysis. GD, PL, SI, LP and DR undertook the statistical analyses. GD and LP wrote the first draft of the paper. All authors contributed to writing the manuscript.

Conflicts of interest

LP reports personal fees from Otsuka Canada, SPMM Course Limited, UK; book royalties from Oxford University Press; investigator-initiated educational grants from Janssen Canada, Otsuka Canada; travel support from Boehringer Ingelheim and Magstim Limited outside the submitted work. In the last 3 years, LP and/or his spouse have held shares in Shire Pharmaceuticals and Glaxo Smith Kline in their pension funds for values less than US$10,000. P F Liddle has received honoraria for academic presentations from Janssen-Cilag and Bristol Myers Squibb; and has taken part in advisory panels for Bristol Myers Squibb. All other authors declare no conflict of interest.

Appendix A. Supplementary data

Supplementary data to this article can be found online at https://doi.org/10.1016/j.schres.2018.01.006.

References

Abler, B., Roebroeck, A., Goebel, R., Hose, A., Schfnfeldt-Lecuona, C., Hole, G., Walter, H., 2006. Investigating directed influences between activated brain areas in a motor-response task using fMRI. Magn. Reson. Imaging 24, 181–185.

Amann, B.L., Canales-Rodríguez, E.J., Madre, M., Radua, J., Monte, G., Alonso-Lana, S., Landin-Romero, R., Moreno-Alcázar, A., Bonnin, C.M., Sarró, S., Ortiz-Gil, J., Gomar, J. J., Moro, N., Fernandez-Corcuera, P., Goikolea, J.M., Blanch, J., Salvador, R., Vieta, E., McKenna, P.J., Pomarol-Clotet, E., 2016. Brain structural changes in schizoaffective disorder compared to schizophrenia and bipolar disorder. Acta Psychiatr. Scand. 133:23–33. https://doi.org/10.1111/acps.12440.

American Psychiatric Association, 1994. Diagnostic and Statistical Manual of Mental Disorders. 4th ed. (Washington D.C).

Argyelan, M., Ikuta, T., Derosse, P., Braga, R.J., Burdick, K.E., John, M., Kingsley, P.B., Malhotra, A.K., Szeszko, P.R., 2013. Resting-state fMRI connectivity impairment in schizophrenia and bipolar disorder. Schizophr. Bull. https://doi.org/10.1093/schbul/sbt092.

Arribas, J.I., Calhoun, V.D., Adali, T., 2010. Automatic Bayesian classification of healthy controls, bipolar disorder, and schizophrenia using intrinsic connectivity maps from FMRI data. IEEE Trans. Biomed. Eng. 57:2850–2860. https://doi.org/10.1109/TBME.2010.2080679.

Ashburner, J., 2007. A fast diffeomorphic image registration algorithm. NeuroImage 38: 95–113. https://doi.org/10.1016/j.neuroimage.2007.07.007.

Baker, J.T., Holmes, A.J., Masters, G.A., Yeo, B.T., Krienen, F., Buckner, R.L., Öngür, D., 2014. Disruption of cortical association networks in schizophrenia and psychotic bipolar disorder. JAMA psychiatry 71 (2), 109–118.

Birur, B., Kraguljac, N.V., Shelton, R.C., Lahti, A.C., 2017. Brain structure, function, and neurochemistry in schizophrenia and bipolar disorder—a systematic review of the magnetic resonance neuroimaging literature. NPJ Schizophr. 3. https://doi.org/10.1038/s41537-017-0013-9.

Bleuler, E., 1950. Dementia Praecox: Or the Group of Schizophrenias (Translated by Zinkin, J.). International Universities Press.

Calhoun, V.D., Maciejewski, P.K., Pearlson, G.D., Kiehl, K.A., 2008. Temporal lobe and "default" hemodynamic brain modes discriminate between schizophrenia and bipolar disorder. Hum. Brain Mapp. 29:1265–1275. https://doi.org/10.1002/hbm.20463.

Calhoun, V.D., Sui, J., Kiehl, K., Turner, J., Allen, E., Pearlson, G., 2012. Exploring the psychosis functional connectome: aberrant intrinsic networks in schizophrenia and bipolar disorder. Front. Neuropsychiatr. Imaging Stimul. 2 (75). https://doi.org/10.3389/fpsyt.2011.00075.

Chai, X.J., Whitfield-Gabrieli, S., Shinn, A.K., Gabrieli, J.D.E., Nieto Castañón, A., McCarthy, J. M., Cohen, B.M., Ongür, D., 2011. Abnormal medial prefrontal cortex resting-state connectivity in bipolar disorder and schizophrenia. Neuropsychopharmacol. 36 (10), 2009–2017.
Chang, C., Glover, G.H., 2009. Effects of model-based physiological noise correction on default mode network anti-correlations and correlations. NeuroImage 47:1448–1459. https://doi.org/10.1016/j.neuroimage.2009.05.012.
Chao-Gan, Y., Yu-Feng, Z., 2010. DPARSF: a MATLAB toolbox for "pipeline" data analysis of resting-state fMRI. Front. Syst. Neurosci. 4.
Costafreda, S.G., Fu, C.H., Picchioni, M., Toulopoulou, T., McDonald, C., Kravariti, E., Walshe, M., Prata, D., Murray, R.M., McGuire, P.K., 2011. Pattern of neural responses to verbal fluency shows diagnostic specificity for schizophrenia and bipolar disorder. BMC Psychiatry 11 (18). https://doi.org/10.1186/1471-244X-11-18.
Craddock, N., Owen, M.J., 2010. The Kraepelinian dichotomy - going, going… but still not gone. Br. J. Psychiatry 196:92–95. https://doi.org/10.1192/bjp.bp.109.073429.
Craddock, R., Holtzheimer, I.P., Hu, X., Mayberg, H., 2009. Disease state prediction from resting state functional connectivity. Magn. Reson. Med. 62 (6), 1619–1628.
Demjaha, A., MacCabe, J.H., Murray, R.M., 2011. How genes and environmental factors determine the different neurodevelopmental trajectories of schizophrenia and bipolar disorder. Schizophr. Bull. https://doi.org/10.1093/schbul/sbr100.
Deshpande, G., Hu, X., 2012. Investigating effective brain connectivity from fMRI data past findings and current issues with reference to granger causality analysis. Brain Connect. 2, 235–245.
Deshpande, G., Hu, X., Stilla, R., Sathian, K., 2008. Effective connectivity during haptic perception: a study using granger causality analysis of functional magnetic resonance imaging data. NeuroImage 40 (4), 1807–1814.
Deshpande, G., LaConte, S., James, G.A., Peltier, S., Hu, X., 2009. Multivariate granger causality analysis of brain networks. Hum. Brain Mapp. 30 (4), 1361–1373.
Deshpande, G., Hu, X., Lacey, S., Stilla, R., Sathian, K., 2010. Object familiarity modulates effective connectivity during haptic shape perception. NeuroImage 49, 1991–2000.
Deshpande, G., Santhanam, P., Hu, X., 2011. Instantaneous and causal connectivity in resting state brain networks derived from functional MRI data. NeuroImage 54 (2), 1043–1052.
Deshpande, G., Sathian, K., Hu, X., Buckhalt, J.A., 2012. A rigorous approach for testing the constructionist hypotheses of brain function. Behav. Brain Sci. 35 (3), 148.
Deshpande, G., Libero, L.E., Sreenivasan, K.R., Deshpande, H.D., Kana, R.K., 2013. Identification of neural connectivity signatures of autism using machine learning. Front. Hum. Neurosci. 7 (670). https://doi.org/10.3389/fnhum.2013.00670.
Ellison-Wright, I., Bullmore, E., 2010. Anatomy of bipolar disorder and schizophrenia: a meta-analysis. Schizophr. Res. 117:1–12. https://doi.org/10.1016/j.schres.2009.12.022.
Feng, C., Deshpande, G., Liu, C., Gu, R., Luo, Y.-J., Krueger, F., 2016. Diffusion of responsibility attenuates altruistic punishment: a functional magnetic resonance imaging effective connectivity study. Hum. Brain Mapp. 37:663–677. https://doi.org/10.1002/hbm.23057.
Fox, M.D., Zhang, D., Snyder, A.Z., Raichle, M.E., 2009. The global signal and observed anticorrelated resting state brain networks. J. Neurophysiol. 101:3270–3283. https://doi.org/10.1152/jn.90777.2008.
Friston, K.J., 1994. Functional and effective connectivity in neuroimaging: a synthesis. Hum. Brain Mapp. 2:56–78. https://doi.org/10.1002/hbm.460020107.
Glahn, D.C., Laird, A.R., Ellison-Wright, I., Thelen, S.M., Robinson, J.L., Lancaster, J.L., Bullmore, E., Fox, P.T., 2008. Meta-analysis of gray matter anomalies in schizophrenia: application of anatomic likelihood estimation and network analysis. Biol. Psychiatry 64:774–781. https://doi.org/10.1016/j.biopsych.2008.03.031.
Glover, G.H., Li, T.Q., Ress, D., 2000. Image-based method for retrospective correction of physiological motion effects in fMRI: RETROICOR. Magn. Reson. Med. 44 (1), 162–167.
Goodyear, K., Parasuraman, R., Chernyak, S., de Visser, E., Madhavan, P., Deshpande, G., Krueger, F., 2017. An fMRI and effective connectivity study investigating miss errors during advice utilization from human and machine agents. Soc. Neurosci. 12: 570–581. https://doi.org/10.1080/17470919.2016.1205131.
Grant, M.M., White, D., Hadley, J., Hutcheson, N., Shelton, R., Sreenivasan, K., Deshpande, G., 2014. Early life trauma and directional brain connectivity within major depression. Hum. Brain Mapp. 35:4815–4826. https://doi.org/10.1002/hbm.22514.
Hampstead, B.M., Stringer, A.Y., Stilla, R.F., Deshpande, G., Hu, X., Moore, A.B., Sathian, K., 2011. Activation and effective connectivity changes following explicit memory training for face-name pairs in patients with mild cognitive impairment: a pilot study. Neurorehabil. Neural Repair 25 (3), 210–222.
Hayasaka, S., 2013. Functional connectivity networks with and without global signal correction. Front. Hum. Neurosci. 7. https://doi.org/10.3389/fnhum.2013.00880.
Huang, G.-B., Wang, D.H., Lan, Y., 2011. Extreme learning machines: a survey. Int. J. Mach. Learn. Cybern. 2 (2), 107–122.
Hutcheson, N.L., Sreenivasan, K.R., Deshpande, G., Reid, M.A., Hadley, J., White, D.M., Ver Hoef, L., Lahti, A.C., 2015. Effective connectivity during episodic memory retrieval in schizophrenia participants before and after antipsychotic medication. Hum. Brain Mapp. 36:1442–1457. https://doi.org/10.1002/hbm.22714.
Iwabuchi, S., Liddle, P.F., Palaniyappan, L., 2013. Clinical utility of machine learning approaches in schizophrenia: improving diagnostic confidence for translational neuroimaging. Front. Neuropsychiatr. Imaging Stimul. 4:95. https://doi.org/10.3389/fpsyt.2013.00095.
James, G., Witten, D., Hastie, T., Tibshirani, R., 2013. Statistical learning. In: An introduction to statistical learning. 112. Springer, New York.
Ketter, T.A., Wang, P.W., Becker, O.V., Nowakowska, C., Yang, Y., 2004. Psychotic bipolar disorders: dimensionally similar to or categorically different from schizophrenia? J. Psychiatr. Res. 38:47–61. https://doi.org/10.1016/S0022-3956(03)00099-2.
Koutsouleris, N., Meisenzahl, E.M., Borgwardt, S., Riecher-Rössler, A., Frodl, T., Kambeitz, J., Köhler, Y., Falkai, P., Möller, H.-J., Reiser, M., Davatzikos, C., 2015. Individualized differential diagnosis of schizophrenia and mood disorders using neuroanatomical biomarkers. Brain J. Neurol. 138:2059–2073. https://doi.org/10.1093/brain/awv111.
Krueger, F., Landgraf, S., Van der Meer, E., Deshpande, G., Hu, X., 2011. Effective connectivity of the multiplication network: a functional MRI and multivariate granger causality mapping study. Hum. Brain Mapp. 32 (9), 1419–1431.
Lacey, S., Hagtvedt, H., Patrick, V.M., Anderson, A., Stilla, R., Deshpande, G., Hu, X., Sato, J.R., Reddy, S., Sathian, K., 2011. Art for reward's sake: visual art recruits the ventral striatum. NeuroImage 55 (1), 420–433.
Landin-Romero, Ramón, Canales-Rodríguez, Erick J., Kumfor, Fiona, Moreno-Alcázar, Ana, Madre, Mercè, Maristany, Teresa, Pomarol-Clotet, Edith, Amann, Benedikt L., 2017. Surface-based brain morphometry and diffusion tensor imaging in schizoaffective disorder. Aust. N. Z. J. Psychiatry 51:42–54. https://doi.org/10.1177/0004867416631827.
Leckman, J.F., Sholomskas, D., Thompson, D., Belanger, A., Weissman, M.M., 1982. Best estimate of lifetime psychiatric diagnosis: a methodological study. Arch. Gen. Psychiatry 39 (8), 879–883.
Liang, P., Li, Z., Deshpande, G., Wang, Z., Hu, X., Li, K., 2014. Altered causal connectivity of resting state brain networks in amnesic MCI. PLoS One 9, e88476. https://doi.org/10.1371/journal.pone.0088476.
Libero, L.E., DeRamus, T.P., Lahti, A.C., Deshpande, G., Kana, R.K., 2015. Multimodal neuroimaging based classification of autism spectrum disorder using anatomical, neurochemical, and white matter correlates. Cortex J. Devoted Study Nerv. Syst. Behav. 66:46–59. https://doi.org/10.1016/j.cortex.2015.02.008.
Lichtenstein, P., Yip, B.H., Björk, C., Pawitan, Y., Cannon, T.D., Sullivan, P.F., Hultman, C.M., 2009. Common genetic determinants of schizophrenia and bipolar disorder in Swedish families: a population-based study. Lancet 373:234–239. https://doi.org/10.1016/S0140-6736(09)60072-6.
Liddle, P.F., Ngan, E.T., Duffield, G., Kho, K., Warren, A.J., 2002. Signs and symptoms of psychotic illness (SSPI): a rating scale. Br. J. Psychiatry 180 (1), 45–50.
Madre, M., Canales-Rodríguez, E.J., Ortiz-Gil, J., Murru, A., Torrent, C., Bramon, E., Perez, V., Orth, M., Brambilla, P., Vieta, E., Amann, B.L., 2016. Neuropsychological and neuroimaging underpinnings of schizoaffective disorder: a systematic review. Acta Psychiatr. Scand. 134:16–30. https://doi.org/10.1111/acps.12564.
Maggioni, E., Crespo-Facorro, B., Nenadic, I., Benedetti, F., Gaser, C., Sauer, H., Roiz-Santiañez, R., Poletti, S., Marinelli, V., Bellani, M., Perlini, C., Ruggeri, M., Altamura, A.C., Diwadkar, V.A., Brambilla, P., ENPACT Group, 2017. Common and distinct structural features of schizophrenia and bipolar disorder: the European network on psychosis, affective disorders and cognitive trajectory (ENPACT) study. PLoS One 12, e0188000. https://doi.org/10.1371/journal.pone.0188000.
Mamah, D., Barch, D.M., Repovš, G., 2013. Resting state functional connectivity of five neural networks in bipolar disorder and schizophrenia. J. Affect. Disord. https://doi.org/10.1016/j.jad.2013.01.051.
Manoliu, A., Riedl, V., Doll, A., Bauml, J.G., Muhlau, M., Schwerthoffer, D., Scherr, M., Zimmer, C., Forstl, H., Bauml, J., Wohlschlager, A.M., Koch, K., Sorg, C., 2013a. Insular dysfunction reflects altered between-network connectivity and severity of negative symptoms in schizophrenia during psychotic remission. Front. Hum. Neurosci. 7. https://doi.org/10.3389/fnhum.2013.00216.
Manoliu, A., Riedl, V., Zherdin, A., Mühlau, M., Schwerthöffer, D., Scherr, M., Peters, H., Zimmer, C., Förstl, H., Bäuml, J., Wohlschläger, A.M., Sorg, C., 2013b. Aberrant dependence of default mode/central executive network interactions on anterior insular salience network activity in schizophrenia. Schizophr. Bull. https://doi.org/10.1093/schbul/sbt037.
Mathalon, D.H., Ford, J.M., 2012. Neurobiology of schizophrenia: search for the elusive correlation with symptoms. Front. Hum. Neurosci. 6 (136). https://doi.org/10.3389/fnhum.2012.00136.
Menon, V., 2011. Large-scale brain networks and psychopathology: a unifying triple network model. Trends Cogn. Sci. 15:483–506. https://doi.org/10.1016/j.tics.2011.08.003.
Moran, L.V., Tagamets, M.A., Sampath, H., O'Donnell, A., Stein, E.A., Kochunov, P., Hong, L. E., 2013. Disruption of anterior insula modulation of large-scale brain networks in schizophrenia. Biol. Psychiatry https://doi.org/10.1016/j.biopsych.2013.02.029.
Murray, R.M., Sham, P., Van Os, J., Zanelli, J., Cannon, M., McDonald, C., 2004. A developmental model for similarities and dissimilarities between schizophrenia and bipolar disorder. Schizophr. Res. 71:405–416. https://doi.org/10.1016/j.schres.2004.03.002.
Nanda, P., Tandon, N., Mathew, I.T., Giakoumatos, C.I., Abhishekh, H.A., Clementz, B.A., Pearlson, G.D., Sweeney, J., Tamminga, C.A., Keshavan, M.S., 2014. Local gyrification index in probands with psychotic disorders and their first-degree relatives. Biol. Psychiatry 76:447–455. https://doi.org/10.1016/j.biopsych.2013.11.018.
Nenadic, I., Maitra, R., Dietzek, M., Langbein, K., Smesny, S., Sauer, H., Gaser, C., 2015a. Prefrontal gyrification in psychotic bipolar I disorder vs. schizophrenia. J. Affect. Disord. 185:104–107. https://doi.org/10.1016/j.jad.2015.06.014.
Nenadic, I., Maitra, R., Langbein, K., Dietzek, M., Lorenz, C., Smesny, S., Reichenbach, J.R., Sauer, H., Gaser, C., 2015b. Brain structure in schizophrenia vs. psychotic bipolar I disorder: a VBM study. Schizophr. Res. 165:212–219. https://doi.org/10.1016/j.schres.2015.04.007.
Nenadić, I., Dietzek, M., Langbein, K., Sauer, H., Gaser, C., 2017a. BrainAGE score indicates accelerated brain aging in schizophrenia, but not bipolar disorder. Psychiatry Res. 266:86–89. https://doi.org/10.1016/j.pscychresns.2017.05.006.
Nenadić, I., Hoof, A., Dietzek, M., Langbein, K., Reichenbach, J.R., Sauer, H., Güllmar, D., 2017b. Diffusion tensor imaging of cingulum bundle and corpus callosum in schizophrenia vs. bipolar disorder. Psychiatry Res. 266:96–100. https://doi.org/10.1016/j.pscychresns.2017.05.011.
Palaniyappan, L., Simmonite, M., White, T.P., Liddle, E.B., Liddle, P.F., 2013. Neural primacy of the salience processing system in schizophrenia. Neuron 79:814–828. https://doi.org/10.1016/j.neuron.2013.06.027.

Palaniyappan, L., Dempster, K., Luo, Q., 2017. A brain network-based grading of psychosis: could resting functional magnetic resonance imaging become a clinical tool? JAMA Psychiatry 74:613–614. https://doi.org/10.1001/jamapsychiatry.2017.0668.

Pettersson-Yeo, W., Allen, P., Benetti, S., McGuire, P., Mechelli, A., 2011. Dysconnectivity in schizophrenia: where are we now? Neurosci. Biobehav. Rev. 35:1110–1124. https://doi.org/10.1016/j.neubiorev.2010.11.004.

Posse, S., Wiese, S., Gembris, D., Mathiak, K., Kessler, C., Grosse-Ruyken, M.-L., Elghahwagi, B., Richards, T., Dager, S.R., Kiselev, V.G., 1999. Enhancement of BOLD-contrast sensitivity by single-shot multi-echo functional MR imaging. Magn. Reson. Med. 42, 87–97.

Preusse, F., Van der Meer, E., Deshpande, G., Krueger, F., Wartenburger, I., 2011. Fluid intelligence allows flexible recruitment of the parieto-frontal network in analogical reasoning. Front. Hum. Neurosci. 5, 22.

Rangaprakash, D., Deshpande, G., Daniel, T.A., Goodman, A.M., Robinson, J.L., Salibi, N., Katz, J.S., Denney, T.S., Dretsch, M.N., 2017. Compromised hippocampus-striatum pathway as a potential imaging biomarker of mild-traumatic brain injury and post-traumatic stress disorder. Hum. Brain Mapp. 38:2843–2864. https://doi.org/10.1002/hbm.23551.

Roebroeck, A., Formisano, E., Goebel, R., 2005. Mapping directed influence over the brain using granger causality and fMRI. NeuroImage 25, 230–242.

Salvador, R., Radua, J., Canales-Rodríguez, E.J., Solanes, A., Sarró, S., Goikolea, J.M., Valiente, A., Monté, G.C., Natividad, M.D.C., Guerrero-Pedraza, A., Moro, N., Fernández-Corcuera, P., Amann, B.L., Maristany, T., Vieta, E., McKenna, P.J., Pomarol-Clotet, E., 2017. Evaluation of machine learning algorithms and structural features for optimal MRI-based diagnostic prediction in psychosis. PLoS One 12, e0175683. https://doi.org/10.1371/journal.pone.0175683.

Sathian, K., Lacey, S., Stilla, R., Gibson, G., Deshpande, G., Hu, X., LaConte, S., Glielmi, C., 2011. Dual pathways for haptic and visual perception of spatial and texture information. NeuroImage 57, 462–475.

Schnack, H.G., Nieuwenhuis, M., van Haren, N.E.M., Abramovic, L., Scheewe, T.W., Brouwer, R.M., Hulshoff Pol, H.E., Kahn, R.S., 2014. Can structural MRI aid in clinical classification? A machine learning study in two independent samples of patients with schizophrenia, bipolar disorder and healthy subjects. NeuroImage 84:299–306. https://doi.org/10.1016/j.neuroimage.2013.08.053.

Seeley, W.W., Menon, V., Schatzberg, A.F., Keller, J., Glover, G.H., Kenna, H., Reiss, A.L., Greicius, M.D., 2007. Dissociable intrinsic connectivity networks for salience processing and executive control. J. Neurosci. 27:2349–2356. https://doi.org/10.1523/JNEUROSCI.5587-06.2007.

Sheffield, J.M., Kandala, S., Tamminga, C.A., Pearlson, G.D., Keshavan, M.S., Sweeney, J.A., Clementz, B.A., Lerman-Sinkoff, D.B., Hill, S.K., Barch, D.M., 2017. Transdiagnostic associations between functional brain network integrity and cognition. JAMA Psychiatry 74:605–613. https://doi.org/10.1001/jamapsychiatry.2017.0669.

Sridharan, D., Levitin, D.J., Menon, V., 2008. A critical role for the right fronto-insular cortex in switching between central-executive and default-mode networks. Proc. Natl. Acad. Sci. 105:12569–12574. https://doi.org/10.1073/pnas.0800005105.

Strenziok, M., Krueger, F., Deshpande, G., Lenroot, R., van der Meer, E., Grafman, J., 2011. Fronto-parietal regulation of media violence exposure in adolescents: a multi-method study. Soc. Cogn. Affect. Neurosci. 5, 22.

Sui, J., Pearlson, G., Caprihan, A., Adali, T., Kiehl, K.A., Liu, J., Yamamoto, J., Calhoun, V.D., 2011. Discriminating schizophrenia and bipolar disorder by fusing fMRI and DTI in a multimodal CCA+ joint ICA model. NeuroImage 57:839–855. https://doi.org/10.1016/j.neuroimage.2011.05.055.

Taylor, M.A., Shorter, E., Vaidya, N.A., Fink, M., 2010. The failure of the schizophrenia concept and the argument for its replacement by hebephrenia: applying the medical model for disease recognition. Acta Psychiatr. Scand. 122:173–183. https://doi.org/10.1111/j.1600-0447.2010.01589.x.

Wang, Y., Katwal, S., Rogers, B., Gore, J., Deshpande, G., 2017. Experimental validation of dynamic granger causality for inferring stimulus-evoked sub-100 ms timing differences from fMRI. IEEE Trans. Neural Syst. Rehabil. Eng. Publ. IEEE Eng. Med. Biol. Soc. 25:539–546. https://doi.org/10.1109/TNSRE.2016.2593655.

Wheelock, M.D., Sreenivasan, K.R., Wood, K.H., Ver Hoef, L.W., Deshpande, G., Knight, D.C., 2014. Threat-related learning relies on distinct dorsal prefrontal cortex network connectivity. NeuroImage 102 (Pt 2):904–912. https://doi.org/10.1016/j.neuroimage.2014.08.005.

WHO Collaborating Centre for Drug Statistics and Methodology, 2003. Guidelines for ATC Classification and DDD Assignment.

Wu, G.-R., Liao, W., Stramaglia, S., Ding, J.-R., Chen, H., Marinazzo, D., 2013. A blind deconvolution approach to recover effective connectivity brain networks from resting state fMRI data. Med. Image Anal. 17:365–374. https://doi.org/10.1016/j.media.2013.01.003.

Yan, C.-G., Cheung, B., Kelly, C., Colcombe, S., Craddock, R.C., Di Martino, A., Li, Q., Zuo, X.-N., Castellanos, F.X., Milham, M.P., 2013. A comprehensive assessment of regional variation in the impact of head micromovements on functional connectomics. NeuroImage 76:183–201. https://doi.org/10.1016/j.neuroimage.2013.03.004.

Yousef, M., Jung, S., Showe, L.C., Showe, M.K., 2007. Recursive cluster elimination (RCE) for classification and feature selection from gene expression data. BMC Bioinf. 8, 144.